Colloid Polym Sci 278:385–391 (2000)

ORIGINAL CONTRIBUTION

F. O. Holtrup
G. Lieser
K. Müllen

Packing behavior of benzoylterryleneimide in the solid state

Received: 14 June 1999
Accepted: 24 November 1999

F. O. Holtrup · G. Lieser (✉) · K. Müllen
Max-Planck-Institut für Polymerforschung
Ackermannweg 10
D-55128 Mainz, Germany

Abstract The packing behavior of benzoylterryleneimide was determined by X-ray powder and electron diffraction. The latter was applied to a material solidified from a solution after spreading it onto a water surface. By this procedure various nonequilibrium structures were prepared: crystalline lamellae are embedded in a structure of lower order, the texture of which looks similar to a texture seen in rigid liquid-crystalline polymers. The transition between both regimes is gradual. X-ray diffraction was applied to an annealed crystalline powder. The crystalline packing of the dark-blue compound can be described by a monoclinic unit cell with lattice parameters $a = 11.25$ Å, $b = 10.93$ Å, $c = 27.78$ Å, $\beta = 91.0°$, $\rho = 1.38$ g/cm^3 and $Z = 4$ at ambient temperature. In order to enable optimum space-filling, the molecules are arranged parallel two by two with the planes of the aromatic ring systems 3.47 Å apart in centrosymmetrical relation and shifted longitudinally so that the diisopropylphenyl group of one molecule fits into the cavity at the carbonyl oxygen of the adjacent molecule.

Key words Benzoylterryleneimide · Molecular packing · Electron diffraction

Introduction

Ryleneimides have been appreciated for a long time due to their outstanding chemical and optical properties [1]. They are characterized by a brilliant color, strong fluorescence and thermal, chemical and photochemical stability [2]. Beside their application as commercial dyes and pigments [3], they are used in reprographical processes [4], in fluorescence solar collectors [5], in photovoltaic devices [6], in dye lasers [7] and in molecular switches [8].

Recently, we described the synthesis of benzoylterryleneimide **1** by converting bromoperylenedicarboximides **2** into stannane **3** (88%) using bis(tributyltin) followed by a Stille coupling with bromide **4** (73%) and oxidative cyclization of **5** (80%) [9]. The mild stannylation eliminates the necessity for the protection of the sensitive carbonyl groups and for inert conditions.

We have now discovered that **1** can also be synthesized via the complementary route, converting bromobenzanthrone **4** into stannane **6** followed by coupling with **2** and subsequent cyclization of **5** (Scheme 1). This second route gives even better yields and fewer side products. The fact that both ways are successful shows that the reaction is very tolerant to electronic or steric variations [10].

1 is a dark-blue pigment exhibiting very high stability in the solid state (decomposition beyond 460 °C). A sample of **1** incorporated in a polystyrene matrix showed no signs of fading or color change after being irradiated with intense UV light (250–800 nm, 810 W/m^2) for 1000 h. **1** is poorly soluble in most organic solvents, only chlorinated solvents or tetrahydrofuran dissolve **1** to a small extent, giving light-blue, turquoiselike solutions ($\lambda_{max} = 676$ nm). The extreme thermal and photochemical stability of **1** in the solid state roused our interest and led us to examine the state of its mutual order.

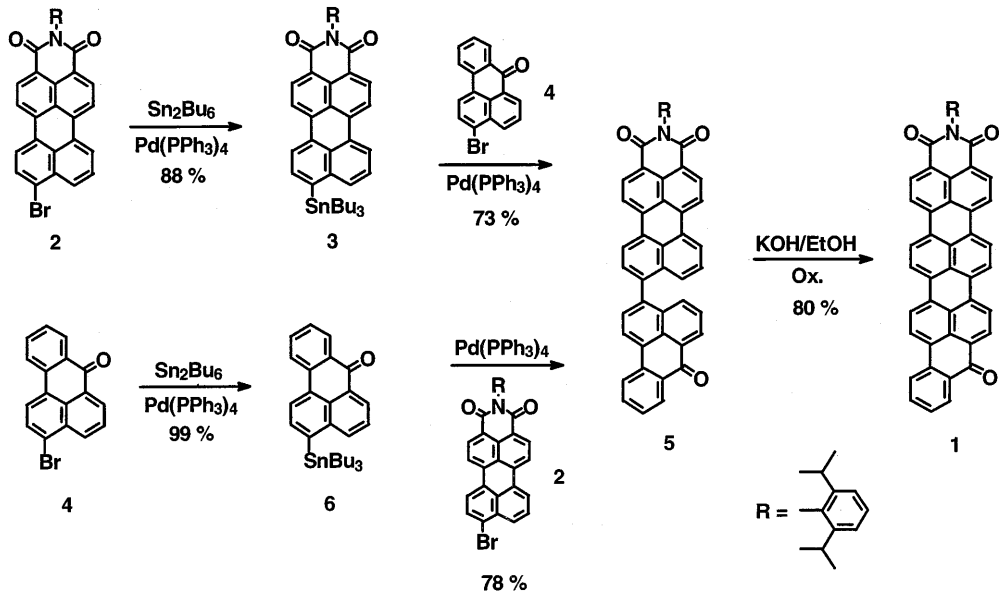

Due to the poor solubility of **1** no large single crystals could be obtained for direct X-ray structure analysis. We started, therefore, from a microcrystalline powder of **1** and tried to approach the crystal structure by the investigation of the packing behavior, taking advantage of a combination of X-ray powder diffraction and electron diffraction.

Experimental

X-ray diffraction

For X-ray investigation we annealed a suspension of the compound in toluene at 70 °C for 5 days under stirring in order to heal structural defects. Subsequently, the powder was filtered and dried. X-ray powder diffraction was performed by means of a Philips PW 1820 diffractometer, using Ni-filtered Cu K_α radiation (λ = 1.5418 Å, 40 kV, 35 mA), scanning a range of $2.0° < 2\theta < 40.0°$ in steps of 0.05°, with 60 s dwell time at each angle.

Electron microscopy and electron diffraction

Some drops of a dilute, yet saturated solution of **1** in tetrachloroethane were spread onto a water surface in a Petri dish. Parts of the thin layer of precipitated solid organic material were transferred from the water surface onto carbon-coated specimen grids. After evaporation of residual solvent the sample was introduced into a transmission electron microscope (TEM) without further preparation, in particular without shadowing with platinum. For both imaging and diffraction a LEO 912 TEM with an integrated Ω electron energy loss spectrometer was used at a high voltage of 120 kV. The diffraction length was calibrated by means of a TlCl powder sample. Series of diffraction patterns, while tilting the crystals, were recorded from irradiated areas with diameters of 1.5 or 2.7 μm. Diffraction patterns were recorded on 35-mm film. For data evaluation, the reflection distances in the diffraction patterns were measured after tenfold magnification in a darkroom magnifier.

Results

On comparing the structural results of X-ray investigation on the one hand and those of electron microscopy and electron diffraction on the other hand one has to take into account that both methods study the same compound, but owing to the different preparation procedures not necessarily the same state of order. From the result of the electron diffraction experiments we see that the state of order is not uniform over the whole sample. In this context it is important to note that the diisopropylphenyl substituent as the only mobile group, *R*, of **1** does not modify the UV/vis spectra significantly when the absorption behavior in organic solvents is compared with the spectra of the compound in the solid state. In both cases the absorption maximum is at the same wavelength of 676 nm [9].

X-ray diffraction

The X-ray powder diagram is displayed in Fig. 1. The very strong maximum at $2\vartheta = 3.2°$, corresponding to a lattice spacing of 27.6 Å, is the innermost of a series of reflections which do not superimpose an amorphous halo of significant intensity. The scattering angles and the corresponding lattice spacings of the observed reflections are listed in Table 1 together with their estimated intensities.

In addition to the X-ray reflections data from electron diffraction experiments are also compiled in Table 1. The indexing of the X-ray peaks in the powder diagram according to the data evaluation of the electron diffraction experiments is not unequivocal, with the only exception being the 001 reflection.

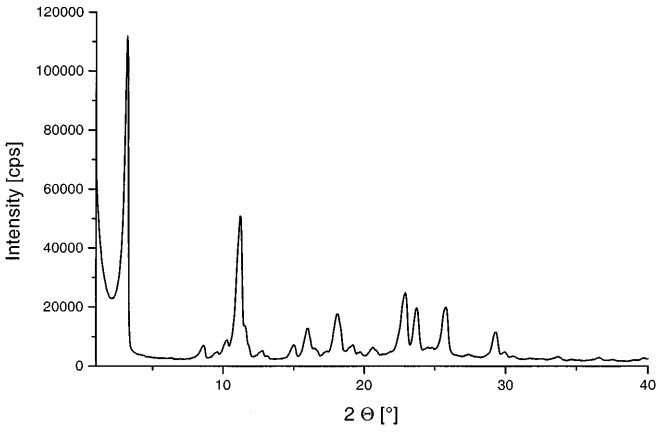

Fig. 1 X-ray powder diffraction diagram of benzoylterryleneimide

Table 1 Reflections from X-ray and electron diffraction experiments. Owing to the preparation used d values of the same $hk\ell$ triple are not fully uniform, resulting in slightly varying lattice parameters. The compiled data stem from a crystal for which the result is independent whether the X-ray 001 reflection is encompassed in the set of data or not. The fact that for higher diffraction angles an X-ray powder reflection is positioned in the same line as an indexed electron diffraction reflection of similar d value does not exclude superposition of several reflections. In some cases only an *asterisk* is inserted. The intensity of the X-ray reflections are indicated as very strong (*vs*), strong (*s*), medium (*m*), weak (*w*), very weak (*vw*) and shoulder (*sh*)

2ϑ (°)	$d_{\text{X-ray}}$ (Å)	Intensity	d_{e^-} (Å)	d_{calc} (Å)	$hk\ell$
3.2	27.6	vs		27.78	001
			11.3	11.25	100
8.6	10.2	m		10.36	101
			10.18	10.17	011
9.6	9.2	m		9.26	003
10.3	8.6	m		8.66	102
				8.59	012
11.2	7.90	vs	7.84	7.84	110
11.6	7.66	sh	7.59	7.57	−111
			7.52	7.50	111
12.8	6.92	m		6.94	004
13.2	6.73	sh		6.79	112
15.0	5.91	m		5.94	113
16.0	5.54	m	5.62	5.62	200
			5.48	5.48	201
			5.42	5.47	020
16.5	5.39	sh	5.38	5.36	021
17.2	5.16	sh		5.18	202
			5.08	5.09	022
			5.00	5.00	210
18.1	4.90	s	4.93	4.91	211
			4.90	4.92	120
			4.80	4.86	121
			4.69	4.68	−212
19.2	4.62	m	4.59	4.62	122
19.7	4.51	w		4.43	−213
20.6	4.31	m		4.36	−123
			3.92	3.92	220
22.9	3.88	s	3.88	3.87	221
23.7	3.75	s	3.77	3.76	222
			3.72	3.71	301
			3.61	3.64	030
24.6	3.63	w	3.59	3.60	302
			3.61	3.59	223
24.8	3.59	w	3.56	3.55	310
			3.55	3.52	032
			3.51	3.51	311
			3.48	3.47	130
25.8	3.45	s	3.46	3.44	−131
			3.45	3.45	−312
			3.43	3.44	131
			3.41	3.42	312
			3.39	3.39	033
			3.36	3.36	132
27.35	3.26	w	3.29	3.29	313
			3.24	3.24	133
			3.08	3.09	320
29.25	3.05	s	3.08	3.07	321
			3.06	3.06	230
			3.02	3.01	322
30.0	2.98	m	2.99	2.98	232
30.5	2.93	w			*
			2.80	2.79	401
			2.74	2.73	040
			2.74	2.75	402
			2.73	2.71	041
			2.68	2.68	042
			2.68	2.68	403
			2.67	2.66	412
			2.66	2.66	140
33.7	2.66	m	2.66	2.64	141
			2.64	2.61	142
34.55	2.60	w	2.61	2.61	330
			2.50	2.51	333
36.55	2.46	m	2.46	2.46	240
37.55	2.40	w	2.37	2.37	243
39.7	2.27	w			*
			2.19	2.21	341
			2.18	2.19	050
			2.14	2.15	150

Electron microscopy

1 is insoluble in water and precipitates immediately when a saturated solution in tetrachloroethane is spread onto a water surface. What was intended originally as a method to get a crystalline specimen thin enough for electron microscopic observation and electron diffraction yielded surprisingly an interesting morphology. Thin lamellae are formed, exhibiting fringes at the lateral boundaries, indicating that the molecular order turns gradually from a crystalline lattice into a state of lower order. Figure 2 shows a lamella surrounded by material of the same compound which adopted textures quite similar to the ones observed in liquid-crystalline polymers with rigid segments [11] or in some prepara-

tions of "hairy-rod" polymers [12], both in lyotropic and thermotropic systems.

Both the lamella and the surrounding material are dichroitic. Viewed in the polarizing microscope with one polarizer only, dichroism makes the rather uniform orientation evident also over large areas with dominating liquid-crystalline texture.

Electron diffraction

An electron diffraction pattern of a lamella like the one in Fig. 2 is displayed in Fig. 3. The lamella is identified as a single crystal. The reflections are spots on an orthogonal (almost square) net.

The dominant feature of the diffraction pattern is the superposition of the diffraction spots of a single crystal and a diffuse annular reflection with some sampling in a limited azimutal region. The annular reflection passes through one pair of spots with a d value of 3.47 Å. The origin of the annular reflection is the less-ordered part of **1**, which forms the liquid-crystalline texture surrounding the crystalline lamella. The diffraction patterns of both regions superimpose because the scattering area was not limited to the crystalline lamella. Electron diffraction thus confirms the different state of order, also making evident that the solid state of low order is transient and cannot resist annealing. In the X-ray powder diagram low order might be seen as an amorphous halo.

If an array of aromatic macrocycles orient their planes in a crystal parallel to each other, a strong reflection belonging to a spacing in the range of 3.47 Å is expected. For the lower order in the rapidly formed and subsequently (after evaporation of the solvent) frozen liquid-crystalline area similar packing of aromatic rings ought to be the origin of a dominant reflection because extended aromatic systems of high electron density probably form lattice planes. Further annular reflections from the region of liquid-crystalline texture are not observed. The intensity of the ring varies as a function of the azimuthal angle, indicating preferential orientation of the molecular moieties. The almost uniform orientation of their dipole moment also gives rise to a maximum of absorption in a preferential direction, visible as dichroism in a polarizing microscope as a function of the orientation of the sample with respect to the vibration plane of the incoming light.

It is worth noting that the strongest reflection of the X-ray powder pattern belonging to a spacing of 27.6 Å is absent in all electron diffraction patterns. Within the whole angular range of beam incidence between $+60°$ and $-60°$ Bragg's reflection condition cannot be fulfilled for the large spacing under the geometrical restrictions of electron diffraction in an electron microscope. This is the second important observation for the derivation of a preliminary picture of molecular packing. The most probable reason for a large spacing in the direction of the incoming beam is the orientation of the molecules inside the crystallite with their largest extension normal or almost normal to the lamellar surface (normal to the supporting carbon film). The length of **1** can be calculated to be 25.7 Å using standard values for bond

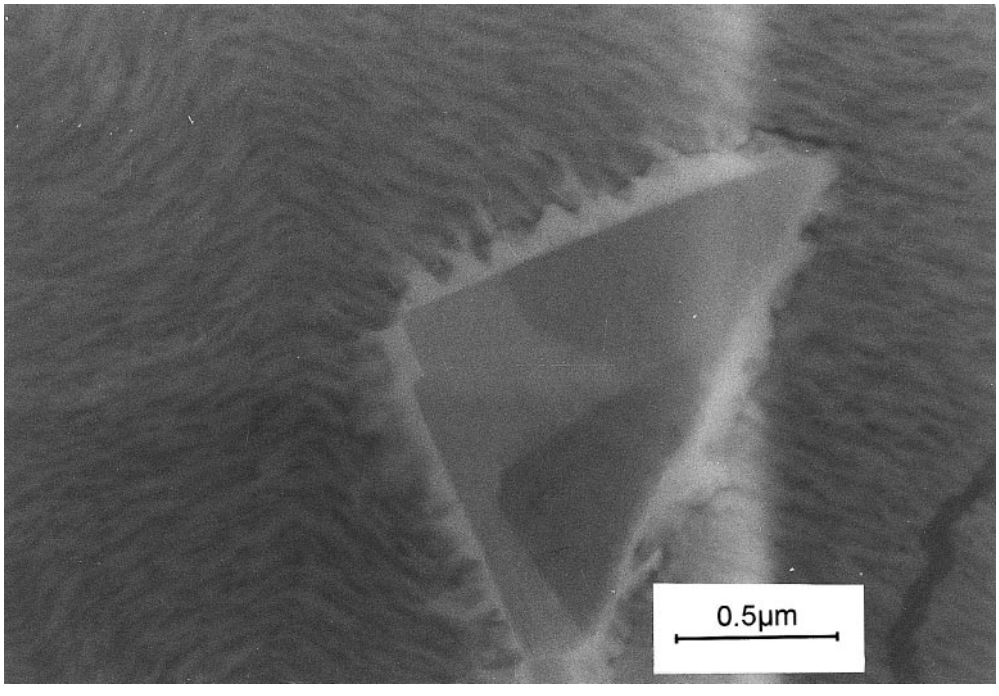

Fig. 2 Electron micrograph of a single crystalline lamella of benzoylterryleneimide. (For the sake of contrast improvement the micrograph was recorded with inelastically scattered electrons at an electron energy loss of $\Delta E = 25$ eV)

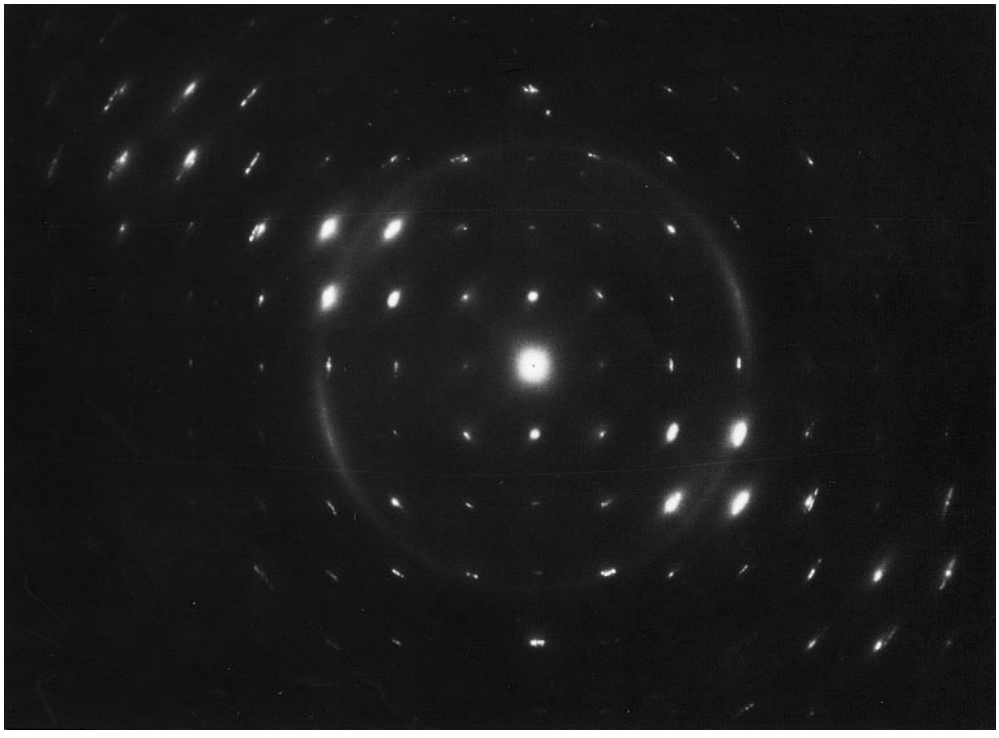

Fig. 3 Electron diffraction pattern of a benzoylterryleneimide lamella. With respect to the incoming beam the crystalline lamella is misoriented to a small degree

lengths and angles (C-C_{ar} 1.4 Å; C-N 1.4 Å; C-H 1.0 Å; vdW_H 1.0 Å). This value is significantly smaller than the observed spacing of 27.6 Å. The discrepancy can be explained by a very frequent pattern of mutual orientation, namely by staggering the molecules with only partial overlap. One could imagine in the actual case that the imide functions of two adjacent molecules are directed in opposite directions with an inversion center. The aromatic parts of the molecules overlap and the diisopropylphenyl groups connected via a single bond stand out in alternate directions on both sides of the stack.

In order to collect diffraction data of various zones the crystal was tilted round distinct axes. (For a short outline of the procedure to determine a unit cell from electron diffraction data see Ref. [13].) During the attempt to find appropriate axes it turned out that the crystalline lattice is monoclinic with an angle β close to 90°. For a monoclinic lattice only tilting round [010] is symmetrical to the (*hk*0) plane (independent of the direction of tilt). After determination of the (*hk*0) plane in reciprocal space the indexing of all observed reflections is unambiguous. It turned out, however, that probably because of the special kind of preparation crystals result, the lattice parameters and consequently the crystallographic density of which vary slightly. In order to decide which crystal is most similar to the annealed crystals used for the X-ray investigation we considered the data set as the best, for which after the refinement of the electron diffraction data the calculated *d* value of the 001 reflection was closest to the observed value in the X-ray experiment.

The electron diffraction data listed in Table 1 originate mainly from two series of zone patterns with [110] as the tilting axis. This was possible because there is only a slight deviation of β from a right angle. Since the lengths of the *a* and *b* lattice parameters do not differ significantly from each other the indexing of the corresponding X-ray powder diffraction data is not possible unambiguously due to multiple superposition of various reflections. From all 00ℓ reflections one can recognize only 001 and 003 without superposition of several reflections. 002 (expected at $2\vartheta = 6.4°$), however, has no significant intensity; whether 004 is present is not unambiguous owing to possible superposition. Appearance of odd 00ℓ and very weak even 00ℓ reflections would point to excess and lack of electrons separated by half of the repeating period of the molecules grouped in pairs with the inversion center [14, 15].

We note in particular that 100 and 010 reflections, expected at $2\vartheta = 7.8°$ and 8.1°, respectively, are absent in the X-ray powder diagram. Whether they appear in the electron diffraction diagrams either due to the loss of symmetry or due to dynamical effects cannot be decided. Dynamical effects are typical for electron diffraction of crystals the thickness of which cannot be controlled. In electron diffraction patterns selection rules are not observed; therefore, a space group cannot be indicated.

Discussion

The formation of single crystals on the one hand and less-ordered liquid-crystalline textures on the other is obviously a function of the kinetics during solidification. One could imagine that the kinetics of the heterogeneous crystallization of **1** from a saturated solution in tetrachloroethane is rapider than the evaporation rate of the solvent. As a consequence, during the proceeding crystallization a state is reached when supersaturation no longer maintains further crystallization, but the concentration of the solution is still high enough to form lyotropic liquid crystals from an anisotropic solution. After complete evaporation the order of the aromatic moieties formed in the liquid-crystalline state is frozen and no further conversion in the crystalline state is possible. To our knowledge, the observation of such textures in low-molecular-weight compounds such as **1** (M = 707 g/mol) is new.

For the crystalline part of the sample a qualitative structural model can de derived by combining X-ray powder data and electron diffraction data: two molecules of **1** are positioned parallel to each other at a distance of 3.47 Å, with the imide groups pointing in opposite directions. The grouping of each pair of molecules is centrosymmetrical and is shifted longitudinally so that the actual overlap of the two molecules corresponds only to a perylene unit.

From the electron diffraction data a monoclinic unit cell is derived with the parameters a = 11.248 ± 0.010 Å, b = 10.931 ± 0.007 Å, c = 27.78 ± 0.19 Å, β = 91.0 ± 0.3° and Z = 4 as result after refinement of 62 independent reflections. With the molecular mass of 707 g/mol a crystallographic density of 1.38 g/cm^3 is calculated. The indicated errors for the lattice parameter

Fig. 4 Molecular model of benzoylterryleneimide molecules in the unit cell, seen from the top (P. Erk, BASF)

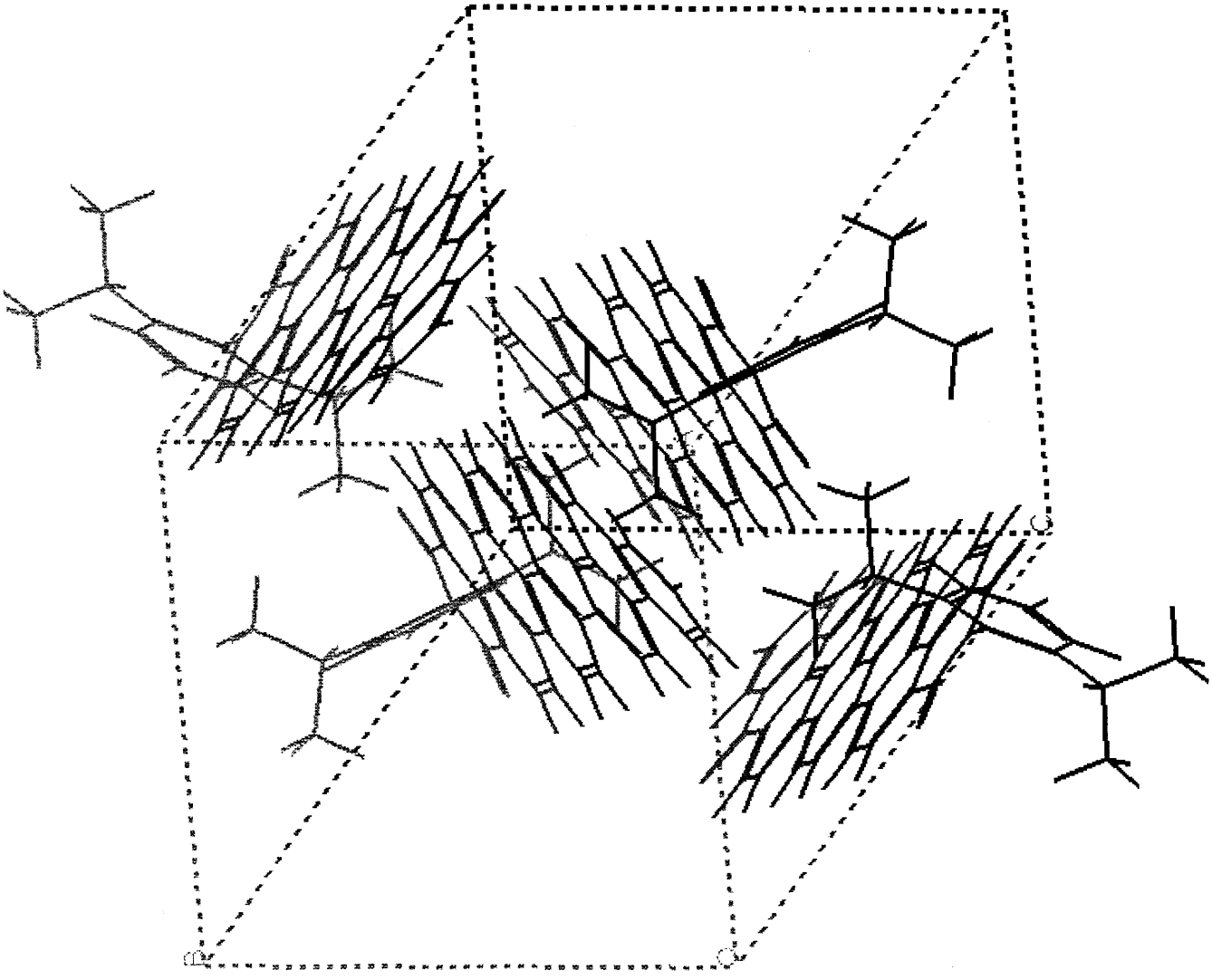

are statistical errors for the data set used. The observed variation of the lattice parameters of different crystals concerns mainly c, leading to a variation of the density between 1.33 and 1.39 g cm^{-3}. The attempt to use a Delaunay reduction for the lattice parameters to find a unit cell of higher symmetry was without success.

Data evaluation shows that the key reflection at d = 3.47 Å has to be indexed by 130, also making evident that the orientation of the extended aromatic system is almost perpendicular to the lamella surface. When the mutual overlap of the plane aromatic parts corresponds only to a perylene unit then mutual gaps are formed behind the nonoverlapping areas in which the isopropyl groups fit above the carbonyl oxygen of the adjacent molecule and the diisopropylphenyl groups can arrange themselves normal to the plane of the terrylene unit, leading to optimum space-filling. This mutual register could explain the high stability of **1** in the solid state (Fig. 4).

The deviations of the packing in the nonequilibrium crystals used for the electron diffraction investigations consist mainly in a shift of both molecules of a pair with respect to each other along the aromatic plane. In the liquid crystal this shift may vary for different molecular pairs in an irregular manner and obviously grants some mobility. After evaporation of the solvent, the liquid-crystalline system freezes in, exhibiting a reflection characterizing the parallel orientation of the aromatic planes in lattice planes. The absence of additional reflections indicates that the crystalline state is not reached.

The unit cell contains another pair of molecules, which has, for the sake of space-filling in the monoclinic cell, essentially the same direction of the molecular axis parallel to c. Ab initio calculations of the molecular packing refined according to Rietveld support this picture of the crystal structure further, indicating that the aromatic planes of the second pair are oriented orthogonal to the plane of the first pair (in {1–30} lattice planes). The application of these modeling methods to **1** will be published by P. Eik, BASF, elsewhere.

Comparing the results with other rylene pigments one can find similarities. The color of perylene diimide pigments is red or black depending on the type of packing [1]. In all cases the molecules form parallel stacks with typical distances of the aromatic ring systems between 3.34 and 3.48 Å. In these stacks the adjacent molecules do not overlap exactly, but are shifted against one another as a function of the sterical demand of the imide substituents. The extent of this shift influences the degree of overlap of the π systems of two adjacent molecules. All black pigments have relatively small or unbranched substituents, allowing an overlap of more than 53%, while the substituents in the red pigments are larger and permit only an overlap of less than 47%.

1 takes a position in-between the two extremes. It has a very bulky substituent (2,6-diisopropylphenyl) standing normal to the terrylene plane; however, since there is only one such substituent per molecule (in contrast to the two imide substituents in perylene diimide), a very close approximation of two adjacent molecules can be achieved. By a longitudinal shift of the two molecules with respect to each other, a centrosymmetrical position is possible allowing an intermolecular distance of 3.47 Å and an overlap of 56% of the aromatic moieties. The filling of space requires that no more than two molecules can be positioned in parallel orientation. Due to the bulkiness of the diisopropylphenyl groups any further molecules can only be positioned normal to the other two. Since **1** cannot form large stacks it absorbs light at exactly the same wavelength in the solid state and in solutions.

Acknowledgements This work was supported by BASF and the Bundesministerium für Bildung und Forschung.

References

1. (a) Graser F, Hädicke E (1980) Liebigs Ann Chem 1994–2011; (b) Graser F, Hädicke E (1984) 483–494
2. Nagao Y, Misono T (1984) Dyes Pigm 5:171–188
3. Seybold G, Wagenblast G (1980) Dyes Pigm 11:303–317
4. Loufty HO, Hor AM, Kazmaier P, Tam M (1989) J Imaging Sci 33:151–159
5. Langhals H (1980) Nachr Chem Tech Lab 28:716–718
6. Schlettwein D, Wöhrle D, Karmann E, Melville U (1994) Chem Mater 6:3–6
7. Reisfeld R, Seybold G (1990) Chimia 44:295–297
8. O' Neil MP, Niemczyk MP, Svec WA, Gosztola D, Gaines GL III, Wasielewski MR (1992) Science 257:63–65
9. Holtrup FO, Müller GRJ, Quante H, De Feyter S, De Schryver FC, Müllen K (1997) Chem Eur J 3:219–225
10. Holtrup FO, Müller GRJ, Uebe J, Müllen K (1997) Tetrahedron 20:6847–6860
11. (a) Thomas EL, Wood BA (1985) Faraday Discuss Chem Soc 79:229–239; (b) Shiwaku T, Nakai A, Hasegawa H, Hashimoto T (1990) Macromolecules 23:1590–1599; (c) Kléman M (1989) Rep Progr Phys 52:555–654; (d) Kléman M (1989) Liq Cryst 5:399–417; (e) Kléman M (1991) In: Ciferri A (ed) Liquid crystallinity in polymers. VCH, Weinheim, pp 365–394
12. (a) Lieser G, Wang W, Albrecht C, Rehahn M, Schwiegk S, Wegner G (1992) Polym Prepr Am Chem Soc Div Polym Chem 33:294–295; (b) Wang W, Lieser G, Wegner G (1993) Liq Cryst 15:1–24; (c) Albrecht C, Lieser G, Wegner G (1993) Prog Colloid Polym Sci 92:111–119; (d) Wang W, Hashimoto T, Lieser G, Wegner G (1994) J Polym Sci Part B Polym Phys 32:2171–2186
13. Fakirov C, Lieser G, Wegner G (1997) Macromol Chem Phys 198:3407–3424
14. Pomerantz M, Segmüller A (1980) Thin Solid Films 68:33–47
15. Rieutord F, Benattar JJ, Bosio L, Robin P, Blot C, de Kouchkovsky R (1987) J Phys 48:679–687